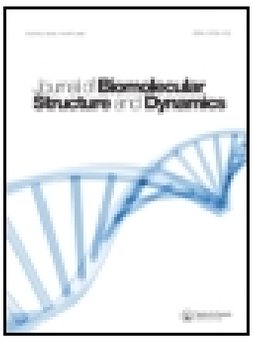

Taylor & Francis
Taylor & Francis Group

Journal of Biomolecular Structure and Dynamics

ISSN: 0739-1102 (Print) 1538-0254 (Online) Journal homepage: https://www.tandfonline.com/loi/tbsd20

Allosteric activation of metabotropic glutamate receptor 5

Balázs Jójárt, Zoltán Orgován, Árpád Márki, Gáspár Pándy-Szekeres, György G. Ferenczy & György M. Keserű

To cite this article: Balázs Jójárt, Zoltán Orgován, Árpád Márki, Gáspár Pándy-Szekeres, György G. Ferenczy & György M. Keserű (2019): Allosteric activation of metabotropic glutamate receptor 5, Journal of Biomolecular Structure and Dynamics, DOI: 10.1080/07391102.2019.1638302

To link to this article: https://doi.org/10.1080/07391102.2019.1638302

JOURNAL OF BIOMOLECULAR STRUCTURE AND DYNAMICS
https://doi.org/10.1080/07391102.2019.1638302

Taylor & Francis
Taylor & Francis Group

Allosteric activation of metabotropic glutamate receptor 5

Balázs Jójárt[a]*, Zoltán Orgován[b]*, Árpád Márki[c], Gáspár Pándy-Szekeres[b], György G. Ferenczy[b] and György M. Keserű[b]

[a]Institute of Food Engineering, University of Szeged, Szeged, Hungary; [b]Medicinal Chemistry Research Group, Research Centre for Natural Sciences, Hungarian Academy of Sciences, Budapest, Hungary; [c]Department of Pharmacodynamics and Biopharmacy, University of Szeged, Szeged, Hungary

Communicated by Ramaswamy H. Sarma

ABSTRACT

Metabotropic glutamate receptor 5 (mGluR5) is a class C G protein-coupled receptor (GPCR) with both an extracellular ligand binding site and an allosteric intrahelical chamber located similarly to the orthosteric ligand binding site of Class A GPCRs. Ligands binding to this ancestral site of mGluR5 can act as positive (PAM), negative (NAM) or silent (SAM) allosteric modulators, and their medicinal chemistry optimization is notoriously difficult, as subtle structural changes may cause significant variation in activity and switch in the functional response. Here we present all atom molecular dynamics simulations of NAM, SAM and PAM complexes formed by closely related ligands and analyse the structural differences of the complexes. Several residues involved in the activation are identified and the formation of a continuous water channel in the active complex but not in the inactive ones is recognized. Our results suggest that the mechanism of mGluR5 activation is similar to that of class A GPCRs.

Abbreviations: MD: molecular dynamics; mGluR5: metabotropic glutamate receptor 5; GPCR: G-protein-coupled receptor; NAM: negative allosteric modulator; PAM: positive allosteric modulator; RMSD: root mean square deviation; SAM: silent allosteric modulator; SAR: structure–activity relationship; SASA: solvent-accessible surface area; TM: transmembrane

ARTICLE HISTORY
Received 13 April 2019
Accepted 24 June 2019

KEYWORDS
Activation mechanism; GPCR; mGluR5; allosteric ligand; activation switches

Introduction

G protein-coupled receptors (GPCR) are a diverse set of seven transmembrane (TM) proteins that mediate various extracellular stimuli to the interior of the cell. They are involved in numerous disorders and their structure and activation mechanism are subject to intensive research. Recent advances in GPCR structural biology together with other experimental and computational tools improved our understanding of the complex mechanism of GPCR activation (Hilger, Masureel, & Kobilka, 2018; Wang, Qiao, & Li, 2018; Weis & Kobilka, 2018). Despite the large variations in GPCR functions, there are common features in their overall structure and activation. Agonist binding induces significant change in the protein conformation, including the positions of the helices, their interactions with each other, with the membrane and with water, and results in the binding to G-protein, and promotes downstream signalling via changes affecting G-protein structure and interactions. In addition, ligand binding to GPCRs may activate β-arrestin-mediated signalling pathways. Metabotropic glutamate (mGlu) receptors (Niswender & Conn, 2010) belong to the class C family of GPCRs. They contain an extracellular domain of glutamate binding site and are able to bind allosteric ligands within the transmembrane domain corresponding to the orthosteric site of class A GPCRs. The mGlu family include eight receptors divided into three groups that act through different intracellular pathways. mGluR5 (Sengmany & Gregory, 2016) belongs to group I whose members are coupled to G_q proteins and activate phospholipase C. The optimization of allosteric mGluR ligands is highly challenging owing to frequently observed steep structure–activity relationships (SAR) and the variation of functional response upon subtle structural changes of the allosteric ligands (molecular switch) (Lindsley et al., 2016). It has been demonstrated recently that steep SAR can be attributed to the flexibility of the allosteric pocket leading to induced binding and to the interaction of the allosteric ligand with the water network in the intrahelical chamber (Christopher et al., 2019).

Computational studies are increasingly applied to explore the structural and dynamical properties of biological macromolecules including GPCRs (Bartuzi, Kaczor, & Matosiuk, 2018; Latorraca, Venkatakrishnan, & Dror, 2017) and among them mGluR receptors (Llinas del Torrent, Pérez-Benito, & Tresadern, 2019). Molecular dynamics (MD) simulations are

CONTACT György M. Keserű keseru.gyorgy@ttk.mta.hu
*Balázs Jójárt and Zoltán Orgován contributed equally to this work.

Supplemental data for this article can be accessed online at https://doi.org/10.1080/07391102.2019.1638302.

particularly valuable in investigating ligand binding (Bernetti, Masetti, Rocchia, & Cavalli, 2019; De Vivo, Masetti, Bottegoni, & Cavalli, 2016; Guo & IJzerman, 2018) and activation mechanism of GPCRs (Miao & McCammon, 2018; Yuan, Chan, et al., 2016; Yuan, Peng, Palczewski, Vogel, & Filipek, 2016). Here we used all-atom MD simulations to examine the effect of closely related allosteric ligands on the structure and activation of the mGluR5 receptor.

Mavoglurant is the prototype of mGluR5 negative allosteric modulators (NAMs), and the replacement of a single Me substituent to Cl and F yields a silent allosteric modulator (SAM) and a positive allosteric modulator (PAM), respectively (Figure 1). Our all atom MD simulations of the transmembrane domains of active and inactive mGluR5 complexes provide information complement to recent experimental structures (Koehl et al., 2019) of the mGluR5 receptor dimer containing extracellular domains. In contrast to the cryo-electron microscopy provided big picture of signal propagation from ligand binding to domain reorganization, our MD simulations focus on changes in the intradomain atomic interactions upon activation and explicitly include the G-protein bound to the active form of the receptor. Previous computational studies on the activation of mGluR receptors include MD simulations for mGluR2 that confirmed the role of the trigger switch amino acids (F643$^{3.40c}$, N735$^{5.47c}$ and W773$^{6.50c}$) in allosteric modulation (Doornbos et al., 2016; Pérez-Benito et al., 2017). MD simulations with mGluR5 NAM and PAM complexes revealed the critical role of the transmission switch residues (S658$^{3.343c}$, Y659$^{3.44c}$ and T781$^{6.46c}$) in allosteric activation (Llinas del Torrent, Casajuana-Martin, Pardo, Tresadern, & Pérez-Benito, 2019). In a recent MD study, dual binding mode of the investigated PAM was found and although elements of the activation mechanism in comparison with class A GPCRS were analysed, limited differences between the hydration of the allosteric sites of active and inactive receptors were observed (Cong, Chéron, Golebiowski, Antonczak, & Fiorucci, 2019). Our MD simulations for the inactive receptor are based on the mavoglurant (NAM) complex for which X-ray structure is available, while the active receptor complex is modelled together with the G_q protein and with a PAM having close structural similarity to mavoglurant. In analysing the results, we pay particular attention to analogy with class A GPCR activation and to the role of water within the allosteric pocket, as water was found to affect both activation in class A GPCRs (Angel, Chance, & Palczewski, 2009; Yuan, Filipek, Palczewski, & Vogel, 2014) and ligand binding in mGluR5 (Christopher et al., 2019).

Simulation of the mavoglurant (NAM)–mGluR5 complex started from the X-ray structure (PDB: 4OO9) (Doré et al., 2014). The complex of the SAM was constructed by replacing the Me group by Cl. The PAM complex was built using the same protein structure with a procedure established for activated class C GPCRs (Doornbos et al., 2016). The TM6 helix was replaced by a model based on the active state μ-opioid receptor in complex with G_i protein (PDB: 6DDE). The G_q protein was modelled using the G_i coordinates of the same complex. The initial position of the PAM ligand was obtained by replacing the Me group by F. 3×500 ns MD simulations were performed for each complex. An additional simulation with mavoglurant (NAM) placed into the active mGluR5 model not containing the G_i protein was also performed to investigate if simulations restore the inactive state.

Methods

Model building

NAM (ID:4OO9) and SAM (ID:4OO9-Cl) complex structures: The 3 D structure of the inactive metabotropic glutamate receptor 5 (mGlu5, PDB code: 4OO9) (Doré et al., 2014) was acquired from Protein Data Bank (Berman et al., 2000) database. The T4-lysozyme which was used to facilitate the crystallization was removed from the structure. The proteins were prepared using default settings of Protein Preparation Wizard (Maestro version: 11.5.011) (Madhavi Sastry, Adzhigirey, Day, Annabhimoju, & Sherman, 2013), the missing loops (ICL 2 (721-728 AA) and ECL 2 (679-688 AA)) were built using Prime ("Schrödinger Release 2018-4, Schrödinger, LLC, New York, NY, 2018," n.d.).

PAM (ID:4OO9-F) structure: The 3 D structure of the inactive metabotropic glutamate receptor 5 (mGlu5, PDB code: 4OO9) (Doré et al., 2014) and the μ-opioid receptor–Gi protein complex (PDB code: 6DDE) (Koehl et al., 2018) were acquired from the Orientations of Proteins in Membranes (OPM) (Lomize, Pogozheva, Joo, Mosberg, & Lomize, 2012) and Protein Data Bank (Berman et al., 2000) databases, respectively. The mGlu5 template contains the Lysozyme coordinates, which were deleted from the file manually (deleted residues: 1–567 and 833–1212).

The sequence of G_q-protein was obtained from the Universal Protein Resource (UniProt ID: P50148) (The UniProt Consortium, 2007).

When combining the mGlu5 and μ-opioid structures, a local structure-based sequence alignment was made for TM6 using GPCRdb generic numbers (Isberg et al., 2015; Pándy-Szekeres et al., 2018). Based on this, three pairs of residues were selected for superimposing the μ-opioid TM6 region (TRP785-TRP293, ILE783-VAL291, THR780-VAL288; 4OO9-6DDE respectively) together with the Gi protein from the μ-opioid–Gi complex structure.

The overall sequence alignment was done by Advanced Homology Modelling package of Schrödinger Suites. The knowledge-based procedure was applied to build 100 multi-template models. The 4OO9 coordinates served as template for the whole receptor except the starting sequence of TM6 (FNEALYIAFTMYTTCI) where the corresponding sequence of 6DDE TM6 (RRITRMVLVVVAVFIV) was the template. The Gq α subunit structure was generated using Gi α subunit coordinates of the 6DDE complex. The Mavoglurant – co-crystallized ligand of 4OO9 – was also included in the model building. The best model was chosen on the basis of normalized Discrete Optimized Protein Energy score (Shen & Sali, 2006). The chosen model was refined by Protein Preparation Wizard Wizard (Maestro version: 11.5.011) (Madhavi Sastry et al., 2013).

The ligand in the X-ray structure was used for 4OO9, and the 2-methyl group of the phenyl ring was changed to

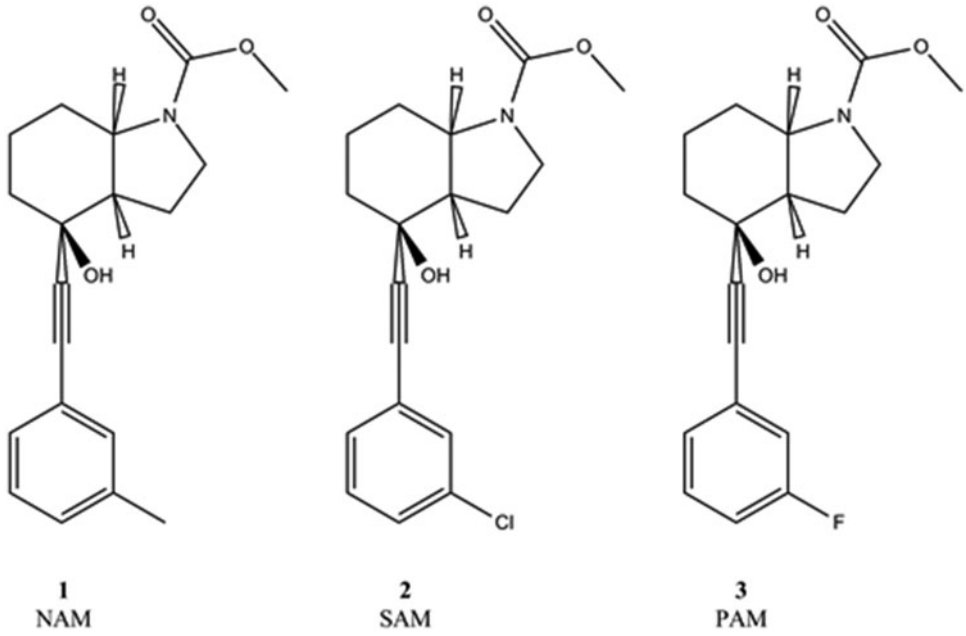

Figure 1. mGlur5 ligands used in the MD simulations.

chloride for creating the SAM, and fluorine for creating the PAM ligands.

Water molecules were generated for each protein cavities using iterative water hot spot identification with molecular interaction field analysis (GRID) (Goodford, 1985; Sciabola et al., 2010) and short molecular dynamics simulations (WaterFLAP version 2.2.1). The energies of the water molecules were calculated using OH2 and CRY (combining C1 and DRY) probes (Mason et al., 2013) and an entropy analysis of the degrees of freedom and the shape of the energy wells of the water molecules.

MD simulation

Molecular dynamics simulations were conducted for three different protein–ligand complexes of the metabotropic glutamate receptor 5. The first one (4OO9) was the crystal structure of the receptor complexed with the negative allosteric modulator, mavoglurant(Doré et al., 2014).The second one was the same structure with a modified ligand (resulted in silent allosteric modulator) where the methyl group was replaced by Cl (4OO9-Cl). The third one was the active state receptor structure with positive allosteric modulator, where the methyl group was replaced by F (ID: 4OO9-F).

The previously prepared structures were placed into fully hydrated POPC membrane by means of the Desmond/System Setup module using the orientation parameters obtained from "Orientations of Proteins in Membranes" website (Lomize et al., 2012). During the preparation the minimum distance between the wall of the periodic box and any protein atoms was set at least 16 Å in the *xy* plane and an additional waterslab was also added in the *z* dimension (15 Å). Appropriate number of ions ($Na+$ and $Cl-$) were added, as well, to ensure a 0.15 mol/dm^3 salt concentration and electroneutrality of the whole system. The number of atoms and the composition of the systems are presented in Table 1.

Table 1. Characteristic parameters of the complex structures investigated by molecular dynamics simulations.

ID	Ligand	N_{atoms}[a]	N_{POPC}[b]	N_W[c]	N_{Na+}[d]	N_{Cl-}[e]
4OO9	NAM	70,846	163	14,866	41	56
4OO9 Cl	SAM	70,855	163	14,880	41	56
4OO9 F	PAM	168,852	314	39,514	110	118

[a]Number of atoms in the whole system.
[b]Number of POPC molecules.
[c]Number of water molecules.
[d]Number of sodium cations.
[e]Number of chloride anions.

After preparation, the membrane protein equilibration protocol was used with GPU code of the DESMOND program package (Bowers et al., 2006), OPLSAA2005 (Banks et al., 2005; Jensen & Jorgensen, 2006; Kaminski, Friesner, Tirado-Rives, & Jorgensen, 2001) parameter set and TIP3P potential for water molecules (Jorgensen et al., 1983). For water molecules present in the initial structure, the Gaussian Barrier Potential was not applied to keep them inside the receptor.

After the equilibration the structure was converted to AMBER format, and the following force field parameters were assigned: protein–ff14SB (Maier et al., 2015), lipid–lipid14 (Dickson et al., 2014), ligand–gaff1.4 (Wang, Wolf, Caldwell, Kollman, & Case, 2004), waters–TIP3P potential, ion–parameters developed by Joung and Cheatham (2008, 2009).

Assignment of gaff1.4 parameters for the ligands was performed with the antechamber (Wang, Wang, Kollman, & Case, 2006) module of AmberTools18 (Case et al., 2018). RESP charges (Dupradeau et al., 2010) were calculated for ligands according to the resp protocol using R.E.D. version III.52 for geometry optimizations and Gaussian 09, Revision A.01 (Frisch et al., 2016) for molecular electrostatic map calculations.

3 × 625-ns-long molecular dynamics simulations were performed for each structure. In the first step, each structure was minimized and two consecutive NVT simulations were conducted at 10 and at 310 K, each step taking 20 ps long.

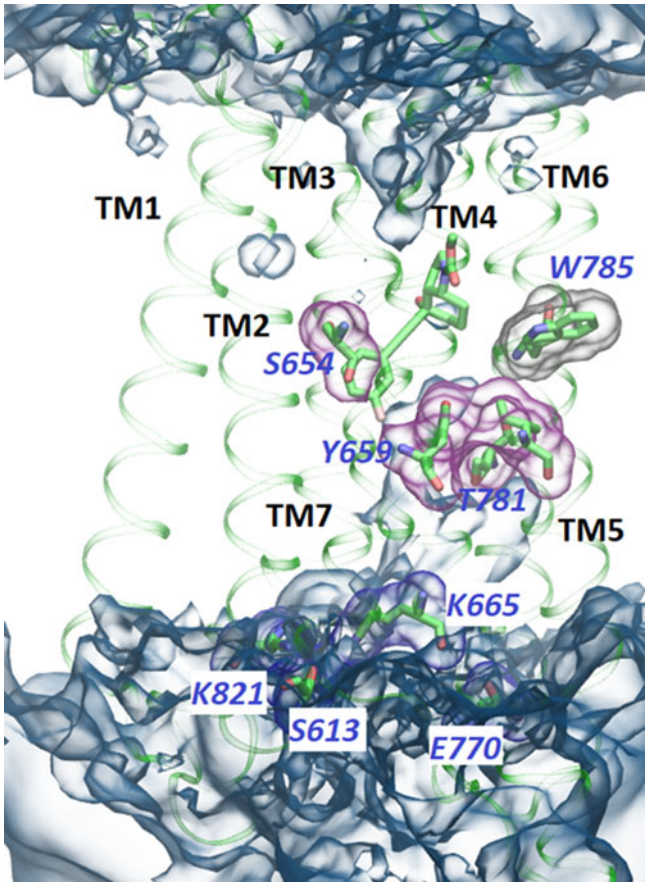

Figure 2. Global view of the TM domain of the PAM complex. Residues found to be involved in activation and discussed in the text are shown. Switch residues Y659$^{3.44c}$, I751$^{5.51c}$ T781$^{6.46c}$ and S654$^{3.39c}$ are shown with grey surfaces. Ionic/polar lock of K665$^{3.50c}$, E770$^{6.35c}$, S613^{ICL1} and K821$^{7.51c}$ is shown with red surfaces and are partially obscured by water. W785$^{6.50c}$ is shown with violet surface. Water is in blue. The water channel under the ligand is characteristic to the PAM complex.

After the NVT calculation, we turned to NPT calculations. The temperature was kept constant using Langevin dynamics (γln = 5.0 ps-1 in NVT and γln = 1.0 ps-1 in NPT) (Bussi & Parrinello, 2007; Melchionna, 2007) and in the NPT step, Berendsen barostat was used (T = 310.0 K, semiisotropic pressure scaling, p = 1.0 bar, τp = 1.0 ps-1, γten = 0.0 dyne/cm, number of interfaces = 2) (Berendsen, Postma, van Gunsteren, DiNola, & Haak, 1984), the cut-off value was set to 10 Å. We applied the hydrogen mass repartition scheme (Hopkins, Le Grand, Walker, & Roitberg, 2015) as well, allowing the use of 4 fs time step.

The GPU version (Götz et al., 2012; Le Grand, Götz, & Walker, 2013; Salomon-Ferrer, Götz, Poole, Le Grand, & Walker, 2013) of pmemd module of AMBER16 (Case et al., 2016) was used in the simulations, achieving 80–90 ns/day and 37 ns/day performance for 4OO9, 4OO9-Cl and 4OO9-F, respectively, with a GeForce GTX 1080 graphics card.

Results and discussion

Complex structures (Figure 2) and binding modes were found to be stable during the simulations (Supplementary Material, Figure S1). The NAM and SAM complexes are very close to the antagonist bound experimental structure (Doré et al., 2014) with a 0.90 Å TM region RMSD. The 2.12 Å TM region RMSD between the PAM complex and the cryo-electron microscopy structure of the active receptor (Koehl et al., 2019) represents a reasonable agreement taking into account that the latter has a 4 Å resolutions and does not include the G-protein (Supplementary Material, Table S1).

A comparative analysis of the MD trajectories of the NAM, SAM and PAM complexes reveals several intriguing differences in the positions, conformations and interactions of the residues (see Figure 2 for an overall view of the TM domain of the PAM complex). Considering the binding site, its solvent-accessible surface area (SASA) in the presence of PAM is larger, and the ~40% increase can be attributed primarily to polar uncharged residues and to a lesser extent to nonpolar residues (Supplementary Material, Figure S2).

W785$^{6.50c}$ was observed to turn transiently towards the ligand in the PAM complex. This is not possible in the complexes of **1** (NAM) and **2** (SAM), as the octahydro-1H-indole group of mavoglurant and its Cl derivative occupies a space would be needed for the indole ring of W785$^{6.50c}$ in the inward position. In the complex of **3** (PAM), however, the outward movement of the TM6 intracellular end makes this rotamer state available, although in our simulation of the active state, it is less populated then the other rotamer pointing away from the allosteric ligand. This highly conserved Trp residue was found to be part of the activation in several class A GPCRs (Trzaskowski et al., 2012), including rhodopsin (Ahuja & Smith, 2009). Nevertheless, its conformational change is not a universal toggle of GPCR activation (Rasmussen et al., 2011), and the conformation is ligand dependent in NAM complexes (Christopher et al., 2015, 2019; Doré et al., 2014) and both conformations are accessible in activated mGluR5 in complex with **3** (PAM).

Y659$^{3.44c}$ is close to the varying aromatic substituent (Me/Cl/F; Scheme 1) of the complexes studied and its analogous 3.40 residue in class A GPCRs is part of the transmission switch (Trzaskowski et al., 2012). Y659$^{3.44c}$ forms either a direct or a water mediated H-bond with T781$^{6.46c}$ in the NAM and SAM complexes. The side chain of Y659$^{3.44c}$ donates an H-bond to the side chain of T781$^{6.46c}$ with an occupancy of 13% (10%) in NAM (SAM) and a water-mediated H-bond is observed with an occupancy of 33% (43%) (Figure 3a). The structural and functional importance of these interactions is underlined by several findings. The water molecule mediating the H-bond between Y659$^{3.44c}$ and T781$^{6.46c}$ is identified in all available X-ray structures of mGluR5-NAM complexes (Christopher et al., 2015, 2019; Doré et al., 2014) and the H-bond was also observed in MD simulations of the mGluR2 (Pérez-Benito et al., 2017) and mGluR5 receptors in complex with NAMs (Llinas del Torrent, Casajuana-Martin, et al., 2019). Moreover, it was shown that mutations of Y659$^{3.44c}$ and T781$^{6.46c}$ in mGluR5 significantly impact the activity of allosteric ligands by either reducing (Gregory et al., 2014; Malherbe et al., 2006) or inverting (Turlington et al., 2013) their functional effect. Our simulations show that this H-bond stabilizes the structure by interconnecting TM3 and TM6. These residues are near to the bottom of the ligand in the intracellular side. Although T781$^{6.46c}$ is located above the

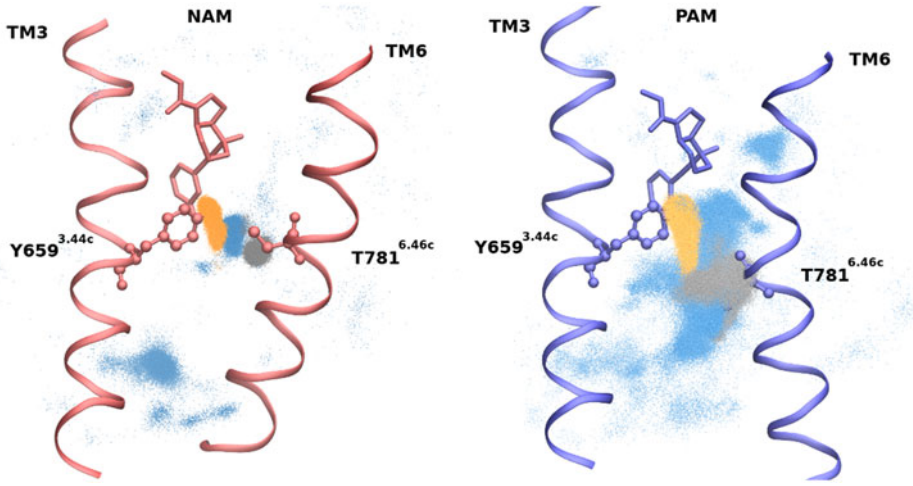

Figure 3. Receptor sidechain positions in NAM and PAM complexes. Distribution of OG1 of T781 (orange), O of Y659 (grey) and water (blue). Direct and water mediated H-bond is characteristic in NAM complex and rare in PAM complex.

kink of TM6, below which TM6 points outward from the helical bundle in the active structure, nevertheless, a ~2Å shift in the backbone atoms of the active structure prevents the formation of a direct H-bond between residues Y659$^{3.44c}$ and T781$^{6.46c}$. A water-mediated H-bond between the side chains is observed only with 7% occupancy, and Y659$^{3.44c}$ donates an H-bond to the backbone of T781$^{6.46c}$ with an occupancy of 13% in the simulations of the PAM complex (Figure 3). Therefore, while the direct and water mediated side chain interactions between these residues tend to fix TM3 and TM6 in the inactive state, the propensity of these structure stabilizing interactions is significantly lower in the active complex resulting in a larger separation of the helices. The increased intrahelical space allows the formation of a continuous water channel from the ligand and Y659$^{3.44c}$ toward the intracellular side of the TM helices (see later). The above mentioned shift of TM6 in the PAM complex leads to the loss of contacts between the ligand and T781$^{6.46c}$ as it is shown by ligand-protein contact probability analysis (Deriu et al., 2014, 2016) (Supplemental Material, Figure S3). Another ligand–protein contact probability significantly differing in NAM and PAM complexes is the one with I621$^{2.46c}$. The contact probability with the methyl group of NAM substantially reduces for the PAM where the methyl group is replaced with an F-atom having smaller van der Waals radius (Supplemental Material, Figure S3).

S654$^{3.39c}$ encloses the intracellular end of the ligand from the opposite side than does Y659$^{3.44c}$ and adopts different conformations in PAM than in NAM and SAM complexes. This residue is adjacent in sequence to P655$^{3.40c}$, the latter is identified as part of the transmission switch in several class A receptors, including histamine H_1 and cannabinoid CB1 receptors (Jongejan et al., 2005; McAllister et al., 2004), and found to play a role in mGluR2 activation (Pérez-Benito et al., 2017). In mGluR5, 3.40c is a proline with limited conformational flexibility. However, the adjacent S654$^{3.39c}$, a residue with ~4 Å separation from the intracellular end of the bound ligand is found to adopt dominantly $g+$ conformation in NAM and SAM complexes, while the t position that has an OH group closer to the ligand and is stabilized by an H-bond to G624$^{2.45c}$ backbone carbonyl is important only in the PAM complex (Supplemental Material, Figure S4).

Ile751$^{5.51c}$ is in contact with Y659$^{3.44c}$ and its analogous 5.51a residue in class A GPCRs is part of the transmission switch. This residue shows distinct conformational preference in PAM versus NAM and SAM complexes (Supplemental Material, Figure S5). While the side chain of Ile751$^{5.51c}$ takes a well-defined conformation with a narrow range of dihedral angles in the NAM complex, it has a larger flexibility in the more opened conformation of the PAM complex. Similar difference for the analogous Ile739$^{5.51c}$ residue was observed for the NAM versus PAM complexes in mGluR2 (Pérez-Benito et al., 2017).

Ionic and polar interactions were observed among residues K665$^{3.50c}$, E770$^{6.35c}$, S613^{ICL1} and K821$^{7.51c}$ in the NAM and SAM complex structures, while they are not representative in the PAM complex (Supplemental Material, Figure S6). These residues correspond to three different helices, TM3, TM6 and TM7, while S613^{ICL1} is the first residue of ICL1 connecting to TM2. The interactions assure close separations for the residues and for the corresponding helices. Analogous locking interactions were observed in the mGluR1 X-ray structure (Wu et al., 2014) and found to be persistent in MD simulations of an inactive mGluR4 model (Dalton, Pin, & Giraldo, 2017). They appear also in $GABA_B$, the other subgroup of class C receptors, and in class A receptors (Binet et al., 2007). However, the distances between the relevant atoms in the PAM complex are significantly higher for each TM pairs, and span a wide range for TM3-TM7, both indicating the loosening of interactions and the critical role of these residues in the activation of both class A and class C GPCRs. Helices TM3, TM6 and TM7 directly interact with G_q, and their interhelical distances at the intracellular side are able to distinguish active from inactive states as it was proposed also for the P2Y1 (class A) receptor(Yuan, Chan, et al., 2016) (Figure 4).

A continuous water channel is observed under the ligand in the PAM complex (Figure 5). No similar water molecules are present in the NAM and SAM complexes (Supplemental Material, Figure S7) owing to the more compact helical

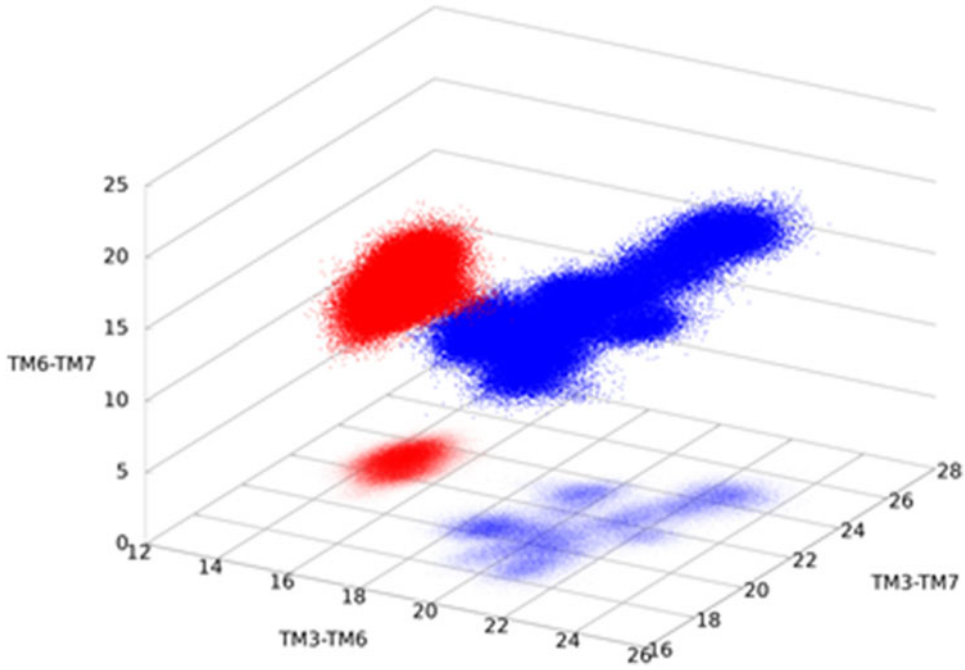

Figure 4. Interhelix separations distinguish active (blue) from inactive (red) structure. TM3, TM6 and TM7 are in direct contact with the G-protein and their increased separation and surface, characteristic to the active structure, facilitates G-protein binding.

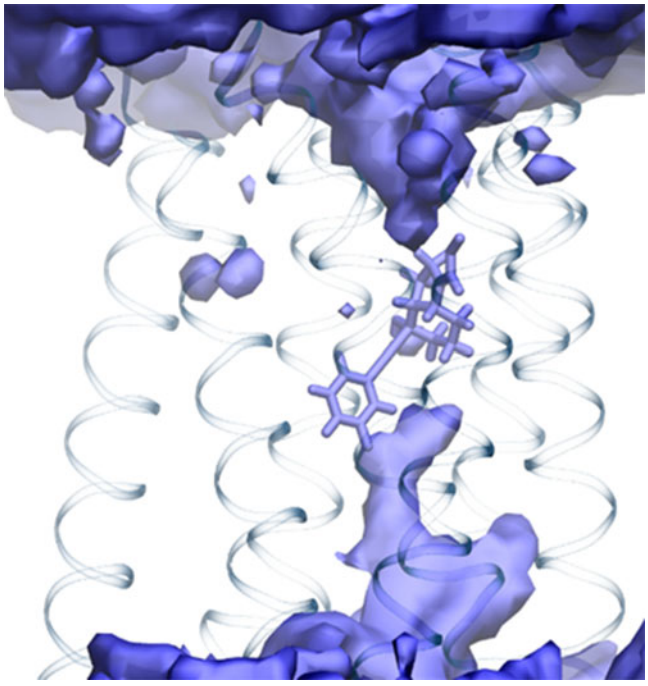

Figure 5. Continuous water channel in the PAM–receptor complex under the ligand at the intracellular side.

bundle in these structures. A comparison of the abundance of water molecules near to the residues in the PAM versus the NAM complexes identifies residues delimiting the water channel in the PAM complex (Supplemental Material, Table S2). L662$^{3.47c}$, A771$^{6.36c}$, I774$^{6.39c}$, T777$^{6.42c}$, M778$^{6.43c}$, T781$^{6.46c}$ and C816$^{7.46c}$ were found to have increased number of neighbouring water molecules and are situated under the ligand toward the cytosolic region. An analogous water channel in class A GPCRs was recognized as a characteristic component of active structures(Angel et al., 2009; Yuan et al., 2014). To check if the formation of the water channel is a distinctive feature of activated mGluR5, an additional MD study was performed in which compound **3** (PAM) in the activated receptor complex was replaced by **1** (NAM) and the G-protein was removed. The water channel disappeared in the simulation and other features of the NAM-complex were restored. In particular, direct and water mediated H-bonds between Y659$^{3.44c}$ and T781$^{6.46c}$, and the ionic and polar interactions among residues K665$^{3.50c}$, E770$^{6.35c}$, S613^{ICL1} and K821$^{7.51c}$ assure close contacts for helices TM3, TM6 and TM7. The SASA of the binding site was reduced to the size previously obtained for the inactive receptor complexed with NAM.

Conclusion

MD simulations expose structural differences between NAM and PAM complexes that are associated with the activation of the mGluR5 receptor. This class C GPCR has a chamber in the TM region where class A receptors have their orthosteric binding site, and this chamber can function as an allosteric site. No endogenous ligand is known to bind to this site, rather it is occupied by water molecules. Our simulations show that the activation of the receptor assisted by a PAM exhibits structural transformations similar to those in class A activation. The backbone movements of TM helices are accompanied by the breaking of interactions like the ionic lock of residues K665$^{3.50c}$, E770$^{6.35c}$, S613^{ICL1} and K821$^{7.51c}$ and the hydrogen bond between Y659$^{3.44c}$ and T781$^{6.46c}$. In addition, residues enclosing the allosteric site, namely, S654$^{3.39c}$ and Y659$^{3.44c}$, both close to the aromatic substituent causing functional switch of the ligands, change their conformation that leads to an increased and more polar chamber. Interestingly, the role of intrahelical waters has not

been investigated in the recent studies (Llinas del Torrent, Casajuana-Martin, Pardo, Tresadern, & Pérez-Benito, 2019). We found that the TM bundle becomes less tightly packed and a continuous water channel is formed among the TM helices in the intracellular side below the PAM, analogously to the formation of a water channel upon activation of class A GPCRs (Angel et al., 2009; Yuan et al., 2014). Moreover, the extended surface created by TM helices, in particular TM3, TM6 and TM7, facilitates G-protein binding leading to signal transduction. These intramolecular changes revealed by the MD simulations contribute to the activation that is also characterized by intermolecular structural rearrangements as observed for mGluR1 (Hlavackova et al., 2012) and mGluR5 (Koehl et al., 2019) receptors.

Residues showing characteristic structural differences in the NAM and PAM complex structures are recognized as part of the activation mechanism. These residues are sequentially and spatially close to or identical with the analogous switches identified in class A receptors as key residues in the activation process (Binet et al., 2007; Nygaard, Frimurer, Holst, Rosenkilde, & Schwartz, 2009; Trzaskowski et al., 2012). Our comparative MD simulations of mGluR5 complexes with NAM, SAM and PAM ligands strongly suggest that mGluR5 activation proceeds via similar changes in residue interactions and the activation mechanism of class A receptors is preserved at a large extent in mGluR5.

Acknowledgements

The support of the National Brain Research Program (KTIA_NAP_13-1-2013-0001 and 2017-1.2.1-NKP-2017-00002) for O. Z., G.G.F. and G.M.K. is acknowledged.

Disclosure statement

No potential conflict of interest was reported by the authors.

ORCID

György G. Ferenczy http://orcid.org/0000-0002-5771-4616
György M. Keserű http://orcid.org/0000-0003-1039-7809

References

Ahuja, S., & Smith, S. O. (2009). Multiple switches in G protein-coupled receptor activation. *Trends in Pharmacological Sciences*, *30*(9), 494–502. doi:10.1016/j.tips.2009.06.003

Angel, T. E., Chance, M. R., & Palczewski, K. (2009). Conserved waters mediate structural and functional activation of family A (rhodopsin-like) G protein-coupled receptors. *Proceedings of the National Academy of Sciences*, *106*(21), 8555–8560. doi:10.1073/pnas.0903545106

Banks, J. L., Beard, H. S., Cao, Y., Cho, A. E., Damm, W., Farid, R., … Levy, R. M. (2005). Integrated modeling program, applied chemical theory (IMPACT). *Journal of Computational Chemistry*, *26*(16), 1752–1780. doi:10.1002/jcc.20292

Bartuzi, D., Kaczor, A. A., & Matosiuk, D. (2018). Opportunities and challenges in the discovery of allosteric modulators of GPCRs. *Methods in Molecular Biology* (Clifton, N.J.), *1705*, 297–319. doi:10.1007/978-1-4939-7465-8_13

Berendsen, H. J. C., Postma, J. P. M., van Gunsteren, W. F., DiNola, A., & Haak, J. R. (1984). Molecular dynamics with coupling to an external bath. *The Journal of Chemical Physics*, *81*(8), 3684–3690. doi:10.1063/1.448118

Berman, H. M., Westbrook, J., Feng, Z., Gilliland, G., Bhat, T. N., Weissig, H., … Bourne, P. E. (2000). The Protein Data Bank. *Nucleic Acids Research*, *28*(1), 235–242. doi:10.1093/nar/28.1.235

Bernetti, M., Masetti, M., Rocchia, W., & Cavalli, A. (2019). Kinetics of drug binding and residence time. *Annual Review of Physical Chemistry*, *70*(1), 143–171. doi:10.1146/annurev-physchem-042018-052340

Binet, V., Duthey, B., Lecaillon, J., Vol, C., Quoyer, J., Labesse, G., … Prézeau, L. (2007). Common structural requirements for heptahelical domain function in class A and class C G protein-coupled receptors. *Journal of Biological Chemistry*, *282*(16), 12154–12163. doi:10.1074/jbc.M611071200

Bowers, K. J., Chow, E. C., Xu, H., Dror, R. O., Eastwood, M. P., Gregersen, B. A., … Sacerdoti, F. D. (2006). Scalable algorithms for molecular dynamics simulations on commodity clusters. In Proceedings of the ACM/IEEE Conference on Supercomputing (SC06).

Bussi, G., & Parrinello, M. (2007). Accurate sampling using Langevin dynamics. *Physical Review E*, *75*(5), 056707. doi:10.1103/PhysRevE.75.056707

Case, D. A., Ben-Shalom, I. Y., Brozell, S. R., Cerutti, D. S., T.E. Cheatham, I., Cruzeiro, V. W. D., … Kollman, P. A. (2018). *AMBER 2018*. San Francisco, CA: University of California.

Case, D., M. Betz, R., Cerutti, D. S., Cheatham, T., Darden, T., Duke, R., … A. Kollman, P. (2016). *AMBER 2016*. San Francisco, CA: University of California.

Christopher, J. A., Aves, S. J., Bennett, K. A., Doré, A. S., Errey, J. C., Jazayeri, A., … Congreve, M. (2015). Fragment and structure-based drug discovery for a class C GPCR: Discovery of the mGlu5 negative allosteric modulator HTL14242 (3-chloro-5-[6-(5-fluoropyridin-2-yl)pyrimidin-4-yl]benzonitrile). *Journal of Medicinal Chemistry*, *58*(16), 6653–6664. doi:10.1021/acs.jmedchem.5b00892

Christopher, J. A., Orgován, Z., Congreve, M., Doré, A. S., Errey, J. C., Marshall, F. H., … Keserű, G. M. (2019). Structure-based optimization strategies for G protein-coupled receptor (GPCR) allosteric modulators: A case study from analyses of new metabotropic glutamate receptor 5 (mGlu 5) X- ray structures. *Journal of Medicinal Chemistry*, *62*(1), 207–222. doi:10.1021/acs.jmedchem.7b01722

Cong, X., Chéron, J.-B., Golebiowski, J., Antonczak, S., & Fiorucci, S. (2019). Allosteric modulation mechanism of the $mGluR_5$ transmembrane domain. *Journal of Chemical Information and Modeling*, *59*(6), 2871. doi:10.1021/acs.jcim.9b00045

Dalton, J. A. R., Pin, J. P., & Giraldo, J. (2017). Analysis of positive and negative allosteric modulation in metabotropic glutamate receptors 4 and 5 with a dual ligand. *Scientific Reports*, *7*(1), 1–14. doi:10.1038/s41598-017-05095-5

De Vivo, M., Masetti, M., Bottegoni, G., & Cavalli, A. (2016). Role of molecular dynamics and related methods in drug discovery. *Journal of Medicinal Chemistry*, *59*(9), 4035–4061. doi:10.1021/acs.jmedchem.5b01684

Deriu, M. A., Grasso, G., Licandro, G., Danani, A., Gallo, D., Tuszynski, J. A., & Morbiducci, U. (2014). Investigation of the Josephin domain protein-protein interaction by molecular dynamics. *PLoS ONE*, *9*(9), e108677. doi:10.1371/journal.pone.0108677

Deriu, M. A., Grasso, G., Tuszynski, J. A., Massai, D., Gallo, D., Morbiducci, U., & Danani, A. (2016). Characterization of the AXH domain of Ataxin-1 using enhanced sampling and functional mode analysis. *Proteins: Structure, Function, and Bioinformatics*, *84*(5), 666–673. doi:10.1002/prot.25017

Dickson, C. J., Madej, B. D., Skjevik, Å. A., Betz, R. M., Teigen, K., Gould, I. R., & Walker, R. C. (2014). Lipid14: The Amber lipid force field. *Journal of Chemical Theory and Computation*, *10*(2), 865–879. doi:10.1021/ct4010307

Doornbos, M. L. J., Pérez-Benito, L., Tresadern, G., Mulder-Krieger, T., Biesmans, I., Trabanco, A. A., … Heitman, L. H. (2016). Molecular mechanism of positive allosteric modulation of the metabotropic glutamate receptor 2 by JNJ-46281222. *British Journal of Pharmacology*, *173*(3), 588–600. doi:10.1111/bph.13390

Doré, A. S., Okrasa, K., Patel, J. C., Serrano-Vega, M., Bennett, K., Cooke, R. M., … Marshall, F. H. (2014). Structure of class C GPCR

metabotropic glutamate receptor 5 transmembrane domain. *Nature*, *511*(7511), 557–562. doi:10.1038/nature13396

Dupradeau, F.-Y., Pigache, A., Zaffran, T., Savineau, C., Lelong, R., Grivel, N., … Cieplak, P. (2010). The R.E.D. tools: Advances in RESP and ESP charge derivation and force field library building. *Physical Chemistry Chemical Physics*, *12*(28), 7821. doi:10.1039/c0cp00111b

Frisch, M. J., Trucks, G. W., Schlegel, H. B., Scuseria, G. E., Robb, M. A., Cheeseman, J. R., … Fox, D. J. (2016). *Gaussian09 Revision A*. Wallingford, CT: Gaussian, Inc.

Goodford, P. J. (1985). A computational procedure for determining energetically favorable binding sites on biologically important macromolecules. *Journal of Medicinal Chemistry*, *28*(7), 849–857. doi:10.1021/jm00145a002

Götz, A. W., Williamson, M. J., Xu, D., Poole, D., Le Grand, S., & Walker, R. C. (2012). Routine microsecond molecular dynamics simulations with AMBER on GPUs. 1. Generalized born. *Journal of Chemical Theory and Computation*, *8*(5), 1542–1555. doi:10.1021/ct200909j

Gregory, K. J., Nguyen, E. D., Malosh, C., Mendenhall, J. L., Zic, J. Z., Bates, B. S., … Conn, P. J. (2014). Identification of specific ligand–receptor interactions that govern binding and cooperativity of diverse modulators to a common metabotropic glutamate receptor 5 allosteric site. *ACS Chemical Neuroscience*, *5*(4), 282–295. doi:10.1021/cn400225x

Guo, D., & IJzerman, A. P. (2018). Molecular basis of ligand dissociation from G protein-coupled receptors and predicting residence time. *Methods in Molecular Biology (Clifton, N.J.)*, *1705*, 197–206. doi:10.1007/978-1-4939-7465-8_9

Hilger, D., Masureel, M., & Kobilka, B. K. (2018). Structure and dynamics of GPCR signaling complexes. *Nature Structural & Molecular Biology*, *25*(1), 4–12. doi:10.1038/s41594-017-0011-7

Hlavackova, V., Zabel, U., Frankova, D., Batz, J., Hoffmann, C., Prezeau, L., … Lohse, M. J. (2012). Sequential inter- and intrasubunit rearrangements during activation of dimeric metabotropic glutamate receptor 1. *Science Signaling*, *5*(237), ra59. doi:10.1126/scisignal.2002720

Hopkins, C. W., Le Grand, S., Walker, R. C., & Roitberg, A. E. (2015). Long-time-step molecular dynamics through hydrogen mass repartitioning. *Journal of Chemical Theory and Computation*, *11*(4), 1864–1874. doi:10.1021/ct5010406

Isberg, V., de Graaf, C., Bortolato, A., Cherezov, V., Katritch, V., Marshall, F. H., … Gloriam, D. E. (2015). Generic GPCR residue numbers – Aligning topology maps while minding the gaps. *Trends in Pharmacological Sciences*, *36*(1), 22–31. doi:10.1016/j.tips.2014.11.001

Jensen, K. P., & Jorgensen, W. L. (2006). Halide, ammonium, and alkali metal ion parameters for modeling aqueous solutions. *Journal of Chemical Theory and Computation*, *2*(6), 1499–1509. doi:10.1021/ct600252r

Jongejan, A., Bruysters, M., Ballesteros, J. A., Haaksma, E., Bakker, R. A., Pardo, L., & Leurs, R. (2005). Linking agonist binding to histamine H1 receptor activation. *Nature Chemical Biology*, *1*(2), 98–103. doi:10.1038/nchembio714

Jorgensen, W. L., Chandrasekhar, J., Madura, J. D., Impey, R. W., Klein, M. L., Chandrasekhar, J., Madura, J. D., … Lein, M. L. (1983). Comparison of simple potential functions for simulating liquid water. *The Journal of Chemical Physics*, *79*(2), 926–935. doi:10.1063/1.445869

Joung, I. S., & Cheatham, T. E. (2008). Determination of alkali and halide monovalent ion parameters for use in explicitly solvated biomolecular simulations. *The Journal of Physical Chemistry B*, *112*(30), 9020–9041. doi:10.1021/jp8001614

Joung, I. S., & Cheatham, T. E. (2009). Molecular dynamics simulations of the dynamic and energetic properties of alkali and halide ions using water-model-specific ion parameters. *The Journal of Physical Chemistry B*, *113*(40), 13279–13290. doi:10.1021/jp902584c

Kaminski, G. A., Friesner, R. A., Tirado-Rives, J., & Jorgensen, W. L. (2001). Evaluation and reparametrization of the OPLS-AA force field for proteins via comparison with accurate quantum chemical calculations on peptides. *The Journal of Physical Chemistry B*, *105*(28), 6474–6487. doi:10.1021/jp003919d

Koehl, A., Hu, H., Feng, D., Sun, B., Zhang, Y., Robertson, M. J., … Kobilka, B. K. (2019). Structural insights into the activation of metabotropic glutamate receptors. *Nature*, *566*(7742), 79–84. doi:10.1038/s41586-019-0881-4

Koehl, A., Hu, H., Maeda, S., Zhang, Y., Qu, Q., Paggi, J. M., … Kobilka, B. K. (2018). Structure of the μ-opioid receptor–Gi protein complex. *Nature*, *558*(7711), 547–552. doi:10.1038/s41586-018-0219-7

Latorraca, N. R., Venkatakrishnan, A. J., & Dror, R. O. (2017). GPCR dynamics: Structures in motion. *Chemical Reviews*, *117*(1), 139–155. doi:10.1021/acs.chemrev.6b00177

Le Grand, S., Götz, A. W., & Walker, R. C. (2013). SPFP: Speed without compromise—A mixed precision model for GPU accelerated molecular dynamics simulations. *Computer Physics Communications*, *184*(2), 374–380. doi:10.1016/j.cpc.2012.09.022

Lindsley, C. W., Emmitte, K. A., Hopkins, C. R., Bridges, T. M., Gregory, K. J., Niswender, C. M., & Conn, P. J. (2016). Practical strategies and concepts in GPCR allosteric modulator discovery: recent advances with metabotropic glutamate receptors. *Chemical Reviews*, *116*(11), 6707–6741. doi:10.1021/acs.chemrev.5b00656

Llinas del Torrent, C., Casajuana-Martin, N., Pardo, L., Tresadern, G., & Pérez-Benito, L. (2019). Mechanisms underlying allosteric molecular switches of metabotropic glutamate receptor 5. *Journal of Chemical Information and Modeling*, *59*(5), 2456–2466. doi:10.1021/acs.jcim.8b00924

Llinas del Torrent, C., Pérez-Benito, L., & Tresadern, G. (2019). Computational drug design applied to the study of metabotropic glutamate receptors. *Molecules (Basel, Switzerland)*, *24*(6), 1098. doi:10.3390/molecules24061098

Lomize, M. A., Pogozheva, I. D., Joo, H., Mosberg, H. I., & Lomize, A. L. (2012). OPM database and PPM web server: Resources for positioning of proteins in membranes. *Nucleic Acids Research*, *40*(D1), D370–D376. doi:10.1093/nar/gkr703

Madhavi Sastry, G., Adzhigirey, M., Day, T., Annabhimoju, R., & Sherman, W. (2013). Protein and ligand preparation: Parameters, protocols, and influence on virtual screening enrichments. *Journal of Computer-Aided Molecular Design*, *27*(3), 221–234. doi:10.1007/s10822-013-9644-8

Maier, J. A., Martinez, C., Kasavajhala, K., Wickstrom, L., Hauser, K. E., & Simmerling, C. (2015). ff14SB: Improving the accuracy of protein side chain and backbone parameters from ff99SB. *Journal of Chemical Theory and Computation*, *11*(8), 3696–3713. doi:10.1021/acs.jctc.5b00255

Malherbe, P., Kratochwil, N., Muhlemann, A., Zenner, M.-T., Fischer, C., Stahl, M., … Porter, R. H. P. (2006). Comparison of the binding pockets of two chemically unrelated allosteric antagonists of the mGlu5 receptor and identification of crucial residues involved in the inverse agonism of MPEP. *Journal of Neurochemistry*, *98*(2), 601–615. doi:10.1111/j.1471-4159.2006.03886.x

Mason, J. S., Bortolato, A., Weiss, D. R., Deflorian, F., Tehan, B., & Marshall, F. H. (2013). High end GPCR design: Crafted ligand design and druggability analysis using protein structure, lipophilic hotspots and explicit water networks. *In Silico Pharmacology*, *1*(1), 23. doi:10.1186/2193-9616-1-23

McAllister, S. D., Hurst, D. P., Barnett-Norris, J., Lynch, D., Reggio, P. H., & Abood, M. E. (2004). Structural mimicry in class A G protein-coupled receptor rotamer toggle switches: The importance of the F3.36(201)/W6.48(357) interaction in cannabinoid CB1 receptor activation. *Journal of Biological Chemistry*, *279*(46), 48024–48037. doi:10.1074/jbc.M406648200

Melchionna, S. (2007). Design of quasisymplectic propagators for Langevin dynamics. *The Journal of Chemical Physics*, *127*(4), 044108. doi:10.1063/1.2753496

Miao, Y., & McCammon, J. A. (2018). Mechanism of the G-protein mimetic nanobody binding to a muscarinic G-protein-coupled receptor. *Proceedings of the National Academy of Sciences*, *115*(12), 3036–3041. doi:10.1073/pnas.1800756115

Niswender, C. M., & Conn, P. J. (2010). Metabotropic glutamate receptors: Physiology, pharmacology, and disease. *Annual Review of Pharmacology and Toxicology*, *50*(1), 295–322. doi:10.1146/annurev.pharmtox.011008.145533

Nygaard, R., Frimurer, T. M., Holst, B., Rosenkilde, M. M., & Schwartz, T. W. (2009). Ligand binding and micro-switches in 7TM receptor

structures. *Trends in Pharmacological Sciences*, *30*(5), 249–259. doi:10.1016/j.tips.2009.02.006

Pándy-Szekeres, G., Munk, C., Tsonkov, T. M., Mordalski, S., Harpsøe, K., Hauser, A. S., … Gloriam, D. E. (2018). GPCRdb in 2018: Adding GPCR structure models and ligands. *Nucleic Acids Research*, *46*(D1), D440–D446. doi:10.1093/nar/gkx1109

Pérez-Benito, L., Doornbos, M. L. J., Cordomí, A., Peeters, L., Lavreysen, H., Pardo, L., & Tresadern, G. (2017). Molecular switches of allosteric modulation of the metabotropic glutamate 2 receptor. *Structure*, *25*(7), 1153–1162.e4. doi:10.1016/j.str.2017.05.021

Rasmussen, S. G. F., Choi, H.-J., Fung, J. J., Pardon, E., Casarosa, P., Chae, P. S., … Kobilka, B. K. (2011). Structure of a nanobody-stabilized active state of the β2 adrenoceptor. *Nature*, *469*(7329), 175–180. doi:10.1038/nature09648

Salomon-Ferrer, R., Götz, A. W., Poole, D., Le Grand, S., & Walker, R. C. (2013). Routine microsecond molecular dynamics simulations with AMBER on GPUs. 2. Explicit solvent particle mesh Ewald. *Journal of Chemical Theory and Computation*, *9*(9), 3878–3888. doi:10.1021/ct400314y

Sciabola, S., Stanton, R. V., Mills, J. E., Flocco, M. M., Baroni, M., Cruciani, G., … Mason, J. S. (2010). High-throughput virtual screening of proteins using GRID molecular interaction fields. *Journal of Chemical Information and Modeling*, *50*(1), 155–169. doi:10.1021/ci9003317

Sengmany, K., & Gregory, K. J. (2016). Metabotropic glutamate receptor subtype 5: Molecular pharmacology, allosteric modulation and stimulus bias. *British Journal of Pharmacology*, *173*(20), 3001–3017. doi:10.1111/bph.13281

Shen, M.-Y., & Sali, A. (2006). Statistical potential for assessment and prediction of protein structures. *Protein Science*, *15*(11), 2507–2524. doi:10.1110/ps.062416606

The UniProt Consortium. (2007). The Universal Protein Resource (UniProt). *Nucleic Acids Research*, *36*(Database), D190–D195. doi:10.1093/nar/gkm895

Trzaskowski, B., Latek, D., Yuan, S., Ghoshdastider, U., Debinski, A., & Filipek, S. (2012). Action of molecular switches in GPCRs–theoretical and experimental studies. *Current Medicinal Chemistry*, *19*(8), 1090–1109. doi:10.2174/092986712799320556

Turlington, M., Noetzel, M. J., Chun, A., Zhou, Y., Gogliotti, R. D., Nguyen, E. D., … Stauffer, S. R. (2013). Exploration of allosteric agonism structure–activity relationships within an acetylene series of metabotropic glutamate receptor 5 ($mGlu_5$) positive allosteric modulators (PAMs): Discovery of 5-((3-fluorophenyl)ethynyl)-*N*-(3-methyloxetan-3-yl)picolinamide (ML254). *Journal of Medicinal Chemistry*, *56*(20), 7976–7996. doi:10.1021/jm401028t

Wang, J., Wang, W., Kollman, P. A., & Case, D. A. (2006). Automatic atom type and bond type perception in molecular mechanical calculations. *Journal of Molecular Graphics and Modelling*, *25*(2), 247–260. doi:10.1016/j.jmgm.2005.12.005

Wang, J., Wolf, R. M., Caldwell, J. W., Kollman, P. A., & Case, D. A. (2004). Development and testing of a general Amber force field. *Journal of Computational Chemistry*, *25*(9), 1157–1174. doi:10.1002/jcc.20035

Wang, W., Qiao, Y., & Li, Z. (2018). New insights into modes of GPCR activation. *Trends in Pharmacological Sciences*, *39*(4), 367–386. doi:10.1016/j.tips.2018.01.001

Weis, W. I., & Kobilka, B. K. (2018). The molecular basis of G protein–coupled receptor activation. *Annual Review of Biochemistry*, *87*(1), 897–919. doi:10.1146/annurev-biochem-060614-033910

Wu, H., Wang, C., Gregory, K. J., Han, G. W., Cho, H. P., Xia, Y., … Stevens, R. C. (2014). Structure of a class C GPCR metabotropic glutamate receptor 1 bound to an allosteric modulator. *Science*, *344*(6179), 58–64. doi:10.1126/science.1249489

Yuan, S., Chan, H. C. S., Vogel, H., Filipek, S., Stevens, R. C., & Palczewski, K. (2016). The molecular mechanism of P2Y1 receptor activation. *Angewandte Chemie International Edition*, *55*(35), 10331–10335. doi:10.1002/anie.201605147

Yuan, S., Filipek, S., Palczewski, K., & Vogel, H. (2014). Activation of G-protein-coupled receptors correlates with the formation of a continuous internal water pathway. *Nature Communications*, *5*(1), 1–10. doi:10.1038/ncomms5733

Yuan, S., Peng, Q., Palczewski, K., Vogel, H., & Filipek, S. (2016). Mechanistic studies on the stereoselectivity of the serotonin 5-HT_{1A} receptor. *Angewandte Chemie International Edition*, *55*(30), 8661–8665. doi:10.1002/anie.201603766